RGSE-Based SPICE Model of Ferrite Core Losses

Alexander Abramovitz, *Member, IEEE*, and Shmuel (Sam) Ben-Yaakov, *Life Fellow, IEEE*

***Abstract*—A SPICE model for estimating and simulating core losses of a ferrite magnetic device is presented. The approach is based on a proposed revised generalized Steinmetz equation (RGSE) and requires only the use of the Steinmetz coefficients and core geometry data. The letter presents a RGSE-based SPICE simulation strategy that can both estimate and simulate the effect of the core losses on the circuit. Primary advantages of RGSE approach are that it does not require switching frequency data and is applicable to arbitrary excitation and not just sinusoidal excitation as the Steinmetz equation approximation does. RGSE model is also insensitive to dc bias, this is an improvement over the earlier model. Comparison of previously reported measured and calculated core loss values with the simulation results of the presented SPICE RGSE model shows excellent agreement in the sinusoidal case and good agreement in the rectangular pulse case.**

***Index Terms*—Core loss, ferrite, ferromagnetic cores, SPICE, Steinmetz equation (SE).**

I. Introduction

FERRITE losses are a limiting factor in an engineering design of high-frequency inductors and transformers. The mechanism of magnetic loss in ferromagnetic material is attributed to hysteresis loss, eddy current loss, and a residual loss [1]. The losses are dependent of the type of the ferrite material, operating frequency, temperature, as well as the waveform and amplitude of the magnetic flux density excitation, and its dc offset value [2]. For this reason, an analytically-based approach for core loss estimation is tedious and difficult, if not impossible, to apply as it requires quite a number of parameters not readily available to the designer in the field [3].

Ferrite core loss data provided in manufacturers' documentation are plots of the (major/static) hysteresis loop and the coefficients of the empirical Steinmetz equation (SE) along with a graphical representation of the fitted SE [4], [5]. Of the two ferrite loss data types, the SE is evidently more useful since it is based on experimental data over the whole practical frequency range and magnetic flux density excitation amplitudes. The fitted SE data are collected under sinusoidal flux density excitation with zero dc bias and for this reason it is strictly valid only under pure ac magnetic flux density excitation. Nonetheless, the empirical SE data are the best, most comprehensive and reliable data available to designers for estimating core losses. However, in most power electronics applications, the inductive components are subjected to rectangular voltage pulses with either variable duty cycle or variable frequency and may carry substantial dc current. Furthermore, discontinuous operation mode entails appearance of zero voltage time intervals. In resonant or quasi resonant converters, the inductor voltage comprises rectangular, sinusoidal, and zero voltage segments and, hence, the magnetic flux density waveform is even more complicated. Therefore, for power electronics practice, the SE loss prediction is not a satisfactory approximation [6]–[8]. To remedy this, a number of previous studies [9]–[21] suggested reformulations and adjustments of the SE to a more realistic operational conditions in which an inductive device is operating under nonsinusoidal but, mainly, rectangular excitation.

Several Steinmetz like models were derived based on the idea that the loss is caused by the rate of change of the flux density, dB/dt, rather than the frequency, f [9]. Among these advanced models are the modified Steinmetz equation (MSE) [10], the generalized Steinmetz equation (GSE) [11], the improved generalized Steinmetz equation (iGSE) [12], the extended Steinmetz equation [13], the improved–improved Steinmetz equation [14] and as well as some others.

Fundamental flaws of the earlier GSE are its inaccuracy when applied to flux density waveforms that include dc bias and its inability to predict the losses during zero voltage intervals (relaxation effect loss). Recently it has been shown that both these problems can be accounted for [14] and [15]. Particularly, core losses in PWM applications were considered in [16] and the rectangular extension of Steinmetz equation [17] was formulated in terms of the duty cycle. The description of Steinmetz parameters (SP) in an extended frequency and temperature range was also suggested in [18]. However, the recent advances [14]–[18] rely on newly defined constants, which are not yet made available to the designers by the manufacturers, and cannot be yet used universally.

The usual CAD tools available to the magnetic designer are SE-based online calculators, provided by major manufacturers, and the ferrite hysteresis models, which were incorporated into a number of electronic circuit simulators including PSPICE and IsSPICE software [22], [23]. The hysteresis model can predict saturation; however, its prediction of loss was never verified rigorously for a wide range of core types and over practical operational conditions such as flux density excitation and temperature range. On the other hand, the SE, which

Manuscript received July 30, 2017; revised September 4, 2017 and October 8, 2017; accepted October 10, 2017. Date of publication October 16, 2017; date of current version January 3, 2018. *(Corresponding Author: Alexander Abramovitz.)*

A. Abramovitz is with the Department of Physical Electronics, Tel Aviv University, Tel Aviv 51100, Israel (e-mail: alabr@hotmail.com).

S. (S.) Ben-Yaakov is with the Department of Electrical and Computer Engineering, Ben-Gurion University, Beersheba 84105, Israel (e-mail: sby@ee.bgu.ac.il).

This paper has supplementary downloadable multimedia material available at http://ieeexplore.ieee.org provided by the authors. This material is 29.9 MB in size.

Color versions of one or more of the figures in this paper are available online at http://ieeexplore.ieee.org.

Digital Object Identifier 10.1109/TPEL.2017.2762759

is more popular among the designers in the field to predict core loss, has hitherto not been formulated into a SPICE model.

This letter introduces a SPICE compatible revised generalized Steinmetz equation (RGSE) model suited for estimating and simulating the core losses of a magnetic device. The proposed RGSE inherits the GSE power to handle a nonsinusoidal magnetic flux excitation but, to avoid the errors of the GSE when dc bias is present, disregards its dc value. By this, the RGSE model mimics the present approach of practicing designers. Clearly, this compromising method is not an ideal one as it does not take into account the relaxation and dc offset effects. But, unlike the present practice, that is valid only for a sinusoidal case, the SPICE compatible RGSE can provide better estimation of the core power loss under nonsinusoidal magnetic flux excitation. Once manufacturers adopt the advanced material characterization procedures and make the new parameters widely available, the proposed RGSE model can be modified to account for the relaxation and dc effects. The proposed RGSE-based SPICE model can be easily incorporated into SPICE schematics of a system that includes inductive elements, such as inductors or transformers, to estimate the expected core loss, and simulate its effect on the circuit.

II. Review of the GSE

An empirical formula (1) that accounts for the combined effect of all core loss factors using a set of only three coefficients is referred to as the SE, which is convenient to apply in practice

$$\overline{P_v} = k f^{\alpha} \hat{B}^{\beta}. \tag{1}$$

Here $\overline{P_v}$ is the time-average power loss per unit volume, f is the excitation frequency, and $\hat{B}$ is the peak amplitude of magnetic flux density. The coefficients k, α, and β are referred to as the SP.

The SPs are obtained by a curve fitting the losses under a sinusoidal magnetic flux density excitation. Accordingly, SE can provide accurate loss estimation only for the sinusoidal case within a certain flux density, frequency, and temperature ranges. However, most of the contemporary power electronic converters operate under pulse width modulation. Magnetic devices in such converters are subject to rectangular voltage excitation. The resultant flux density is a kind of a piecewise linear waveform that also may have a nonzero dc component. For these reasons, the accuracy of SE prediction is compromised.

To account for the realistic operational conditions of magnetic devices found in practical power electronics applications, the GSE approach [11] was suggested. According to the GSE hypothesis the instantaneous power loss function of the core material is

$$P_v(t) = k_1 \left| \frac{dB(t)}{dt} \right|^{\alpha} |B(t)|^{\beta-\alpha} \tag{2}$$

whereas the time-average power loss in the core material per unit volume can be found from

$$\overline{P_v} = \frac{1}{T} \int_0^T P_v(t)\, dt \tag{3}$$

where $T = 1/f$ is the period of the excitation, α, and β are the original SP, and k_1 is related to the Steinmetz parameter *k* by

$$k_1 = \frac{k}{(2\pi)^{\alpha-1} \int_0^{2\pi} |\cos\theta|^{\alpha} |\sin\theta|^{\beta-\alpha} d\theta}. \tag{4}$$

Note that (4) introduces no additional dependence on frequency so that k_1 is a constant.

Indeed, it could be shown that for sinusoidal flux density $B(t) = \hat{B}\sin(\theta)$, $(\theta = 2\pi f t)$, SE (1) is just a private case of GSE model (2)–(4).

GSE authors claimed that GSE is "in most cases, the most useful tool available to magnetics designers who need to predict losses in MnZn ferrites with nonsinusoidal flux waveforms. It gives accurate predictions for a wide range of conditions, and provides a simple way to make these predictions requiring no material characterization beyond the SPs, which are often available from core manufacturers" [11].

While representing a significant improvement over earlier methods, GSE does inherits some of the limitations of the SE such as the limited flux density and frequency range and the temperature dependence of SPs, as well as the dc offset problem. Moreover GSE is rather difficult, if not impossible, to compute "by hand" as (2) and (3) involve tedious integration of time dependent exponential functions.

III. Derivation of the SPICE Compatible Core Loss Model

A. Preliminary Considerations

What is intuitively simple for a human designer can be rather challenging for a circuit simulator and vice versa. Although SE (1) can be implemented in SPICE within a single analog behavioral building block (ABM), additional ABMs are needed to help determine the frequency, *f*, and the peak flux density $\hat{B}$, which also may be time varying. These are rather demanding tasks that require substantial software resources and may introduce time delays. Furthermore, the classical SE is valid only for sinusoidal excitation while flux density waveform of cores in PWM converters is mostly either triangular or trapezoidal. Hence, using SE (1) as a basis for SPICE loss estimation algorithm is disadvantageous. The MSE [10] employs the concept of equivalent frequency that reportedly accounts for the high frequency components of an arbitrary flux density waveform, but poses even more profound difficulties for SPICE implementation.

SPICE circuit simulator preferably works with instantaneous functions and, thus, can attain the numerical solution of (2) and (3) effortlessly. Therefore, an additional merit of GSE formulation, beyond the fact that it is applicable to nonsinusoidal excitation, is that it is SPICE friendly and easily lends itself for implementation in SPICE. However, GSE has a problem, "GSE loss predictions do depend on dc bias, which appears to be significantly greater than that of actual materials" [11]. Since most inductors in power electronic applications do carry dc current the GSE's dc sensitivity problem can significantly impair the accuracy of power loss estimation. This prompted [12] to restate (2) in terms of the ac peak flux density, $\hat{B}$, instead of the instantaneous flux density, *B(t)*. This excludes the dc offset from calculations. The improved model was referred to as the iGSE and was found to be more accurate. Still, due to the difficulties

involved in establishing the peak flux density, $\hat{B}$, iGSE will not be considered here. Instead a related SPICE-friendly modeling approach is developed, as described below.

B. Proposed RGSE Model

The RGSE instantaneous power loss density function can be derived from (2) as

$$P_v\ (t) = k_1 \left|\frac{dB\,(t)}{dt}\right|^{\alpha} |B\,(t) - B_{\rm DC}|^{\beta-\alpha} \tag{5}$$

where $B_{\rm DC}$ is the dc offset (the time average value) of the instantaneous flux density B(t), α and β are the original SP, and k_1 is same as (4).

The idea behind the RGSE (5) is simply disregarding the effect of the flux density dc offset on core loss and considering the contribution of the ac flux density only. Therefore, the dc inflicted errors, inherent to the GSE, are mitigated by the RGSE model. The downside of this approach is that RGSE, same as iGSE, does not correct for the dc bias dependence of the core loss. This compromising approach is still deemed useful considering the commonly applied engineering practices that usually disregard the dc bias effect on the core loss due to the lack of both workable theory and related manufacturer data to account for the dc offset inflicted loss. Worth noting that it was recently verified experimentally [15] that by introducing appropriate correction factors in Steinmetz parameters k and β (α does not depend on dc bias), it is possible to account for the dc bias effect. Once such correction terms would be available from manufacturers then they can be easily incorporated to upgrade the proposed RGSE model.

The proposed RGSE model was identified as a viable candidate to be applied as SPICE loss estimation algorithm due to the following advantages: continuous time SPICE-friendly formulation, uses the available SP, accounts for an arbitrary excitation, and is insensitive to dc offset. Furthermore, under pure sinusoidal excitation the average power loss computed with RGSE by (3) and (5) is identical to that predicted by SE (1).

IV. SPICE Implementation of RGSE-Based Core Loss Estimator

A. Further Considerations

Since SPICE operates with electrical quantities, it is desirable to reformulate the RGSE power loss function (5) in terms of inductor's voltage. Recalling Faraday's law

$$\frac{dB\,(t)}{dt} = -\frac{v\,(t)}{NA_e} \tag{6}$$

the flux density, *B(t)*, in (5) can be recognized as

$$B\ (t) = \frac{1}{NA_e}\int_0^t v\,(t)\,dt \tag{7}$$

whereas the second term in (5) is the ac flux density obtained by disposing of the dc term

$$B_{\rm AC}\ (t) = B\,(t) - B_{\rm DC} = \frac{1}{NA_e}\int_0^t v\,(t)\,dt - \frac{1}{T}\int_{t-T}\left(\frac{1}{NA_e}\int_0^t v\,(t)\,dt\right)dt \tag{8}$$

here *T* is the excitation (averaging) period.

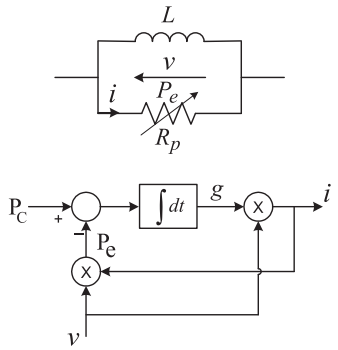

Fig. 1. Current generation scheme of the power controlled resistance.

Plugging (6)–(8) into (5) and manipulating the expression yields

$$P_c\ (t) = V_e k_1 \left|\left(\frac{v\,(t)}{NA_e}\right)^{\alpha} \cdot B_{AC}^{\beta-\alpha}\,(t)\right|. \tag{9}$$

Here A_e is the effective area of the core, V_e is the effective volume of the core, and *N* is the number of turns of the inductor under test.

Time average of (9) yields the desired average core power loss, P_{Cav}, in the specified core.

B. Power Controlled Resistance

Another issue to consider is the translation of the predicted power loss into the simulated circuit. This task can be carried out by a power controlled resistor (PCR), shown in Fig. 1. PCR is configured in parallel with the inductor under test to emulate an equivalent parallel resistor, R_p. The task of PCR is to generate a current, *i(t)*, such that: (a) *i(t)* is a scaled replica of *v(t)* waveform; and (b) drawing same average power from the simulated circuit as predicted by (9).

PCR's principle of current generation can be understood by examining Fig. 1. PCR accepts the instantaneous power loss prediction (9) as the reference signal, $P_c(t)$, as well as the inductor terminals voltage, *v(t)*, and outputs the current $i(t) = g(t)v(t)$ according to the Ohm's law. The transconductance of PCR, $g = 1/R_p$, is determined dynamically, in a closed loop, to adjust to the expected variations in core power loss at different operation conditions according to

$$g\,(t) = \frac{1}{\tau}\int \left(P_c\,(t) - v\,(t)\,i\,(t)\right)dt. \tag{10}$$

Due to integration in (10), the power feedback loop in Fig. 1 is of Type 1 and tends to develop an appropriate current amplitude such as to null the average steady state error signal, $\overline{P_c(t) - v(t)i(t)} = 0$. Therefore, as the steady state is reached, the average power, $\overline{v(t)i(t)}$, absorbed by PCR converges to the average core loss, $\overline{P_c(t)}$, predicted by the RGSE and (b) is fulfilled.

To prevent distortion of the current waveform, and so fulfil (a), the transconductance variable, *g(t)*, is made slowly varying relative to *v(t)*. This is easily achieved by setting $\tau = 1$, which restricts the bandwidth of the feedback loop. Faster response can be achieved with smaller values of τ.

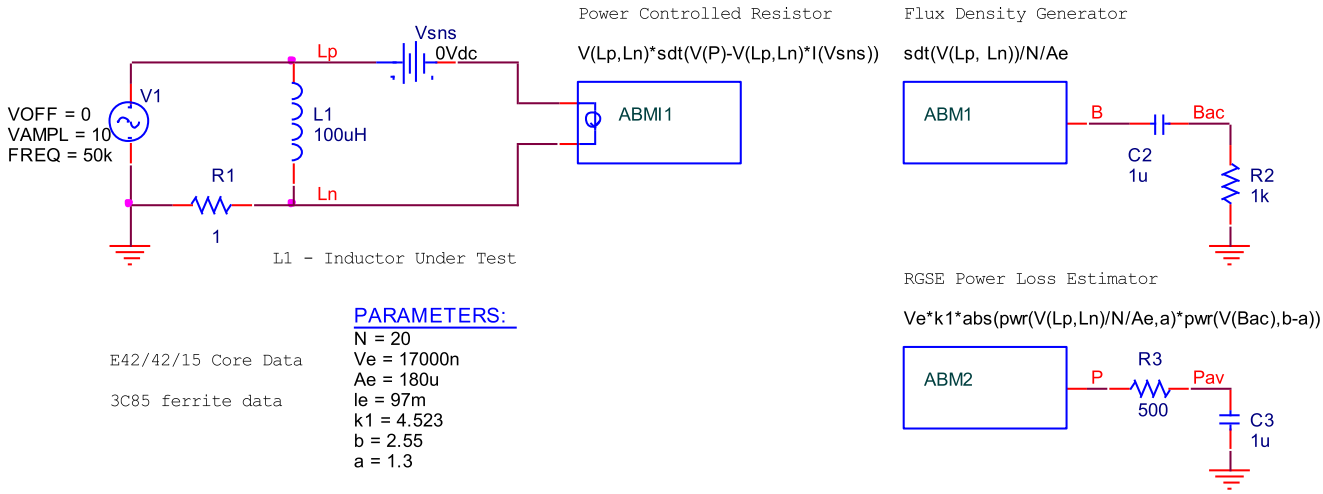

Fig. 2. Schematic diagram of RGSE-based SPICE core loss estimator of L1 inductor core loss under sinusoidal excitation.

C. Simulation Approach

Fig. 2 illustrates the PSPICE schematics needed to evaluate and simulate core loss of an inductor within a simple *RL* circuit, *V*1, *L*1, *R*1. As shown in Fig. 2, only three ABM blocks are required to implement the RGSE-based core loss SPICE model.

In Fig. 2, ABM1 derives the flux density, $B(t)$, according to (7) applying the PSPICE syntax

$$\text{sdt}\left(V\left(Lp,Ln\right)\right)/N/Ae. \tag{11}$$

The required ac flux density (8) is then obtained with a high-pass filter *R*2, *C*2, and coded in voltage, *V*(Bac).

The core power loss is evaluated by ABM1, according to (9), applying PSPICE syntax

$$Ve^{*}k1^{*}\text{abs}\left(\text{pwr}\left(V\left(Lp,Ln\right)/N/Ae,a\right)^{*}\right.$$
$$\left.\times\ \text{pwr}\left(V\left(\text{Bac}\right),b-a\right)\right) \tag{12}$$

which outputs the instantaneous power loss, $P_c(t)$, and coded in voltage, *V*(*P*).

The average power loss is obtained with a low-pass filter *R*3, *C*3, and coded in voltage, *V*(Pav).

Note that the corner frequency of both the high-pass and the low-pass filters has to be chosen at least a decade below the lowest expected excitation frequency in the circuit.

The equivalent parallel resistance, R_p, is realized by ABMI1 employing the PCR scheme in Fig. 1. The output current of ABMI1 is derived by the PSPICE syntax

$$V\left(Lp,Ln\right)^{*}\text{sdt}\left(V\left(P\right)-V\left(Lp,Ln\right)^{*}I\left(V\text{sns}\right)\right) \tag{13}$$

where the transconductance variable (10) is implemented by PSPICE syntax sdt(*V*(*P*)–*V*(*Lp*,*Ln*)**I*(*V*sns)); *I*(*V*sns) is the current of ABMI1 (as measured through *V*sns source); *V*(*Lp*,*Ln*) is the voltage across the inductor; and, accordingly, *V*(*Lp*,*Ln*)**I*(*V*sns) is the electrical power sunken by ABMI1 from the simulated circuit.

Core geometrical data and SPs set are introduced into the program using the PARAM statement. Note that $a=\alpha$, $b=\beta$, and k_1 according to (4) are required by ABM1.

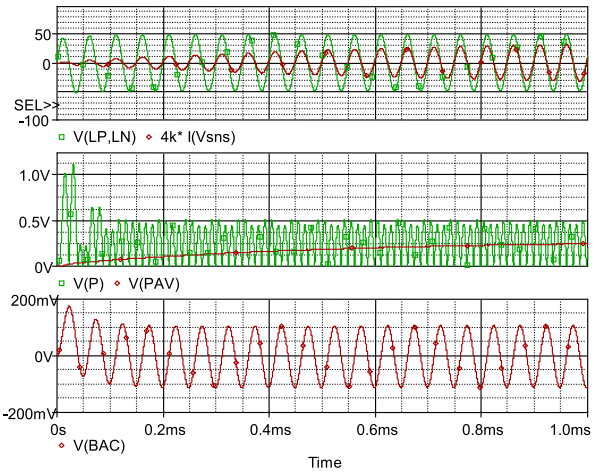

Fig. 3. Typical simulation waveforms of RGSE core power loss estimator under pure sinusoidal excitation. Upper screen–the inductor's voltage, *V*(*LP*,*LN*), and the scaled PCR current, 4k**I*(*V*sns); middle screen- the instantaneous core power loss, *V*(*P*), and the average core power loss, *V*(PAV); bottom screen- the ac flux density, *V*(BAC).

V. Simulation Results

The following simulation experiments were conducted for the core parameters used in [10]: core material 3C85; core size E42/42/15; effective length $l_e = 97$ mm; effective area $A_e = 180$ mm^2; and effective volume $V_e = 17000$ mm^3. The SPs are $k = 12$, $a = 1.33$, and $b = 2.55$. Solving (4) yields $k_1 = 4.523$. In absence of other data, it was assumed that the inductor under test was wound using $N = 20$ turns and that the resulting inductance is $L = 100\,\mu$Hy.

During the first software experiment the core under test (CUT) was excited by a pure sinusoidal flux density as illustrated in Fig. 2. Typical simulated waveforms of the RGSE loss predictions are shown in Fig. 3.

Top screen shows the inductor voltage, *V*(*Lp*,*Ln*), and the scaled PCR current, 4*k***I*(*V*sns), during the start–up transient. Smooth development of the current is observed. The current is in phase with voltage and of identical waveform with no noticeable distortion. This confirms proper function of the PCR. Second

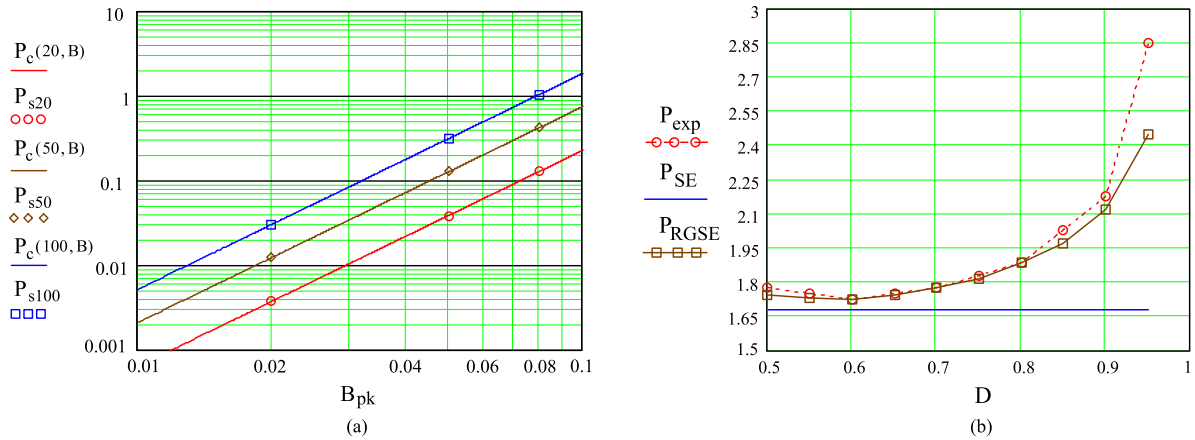

Fig. 4. (a) Comparison of RGSE-based SPICE simulation results (o's dots- P_{s20}, simulated at 20 kHz; diamond dots- P_{s50}, simulated at 50 kHz; box dots- P_{s100}, simulated at 100 kHz;) versus SE calculated results (solid lines: red- P_c(20,B), calculated at 20 kHz; brown-P_c(50,B), calculated at 50 kHz; blue- P_c(100,B), calculated at 100 kHz;) (sinusoidal excitation). (b) Comparison of RGSE-based SPICE simulation results (P_{RGSE}- box) versus SE calculated results (P_{SE} –diamond) versus experimental results (P_{exp}- o's) [10] (pulse excitation).

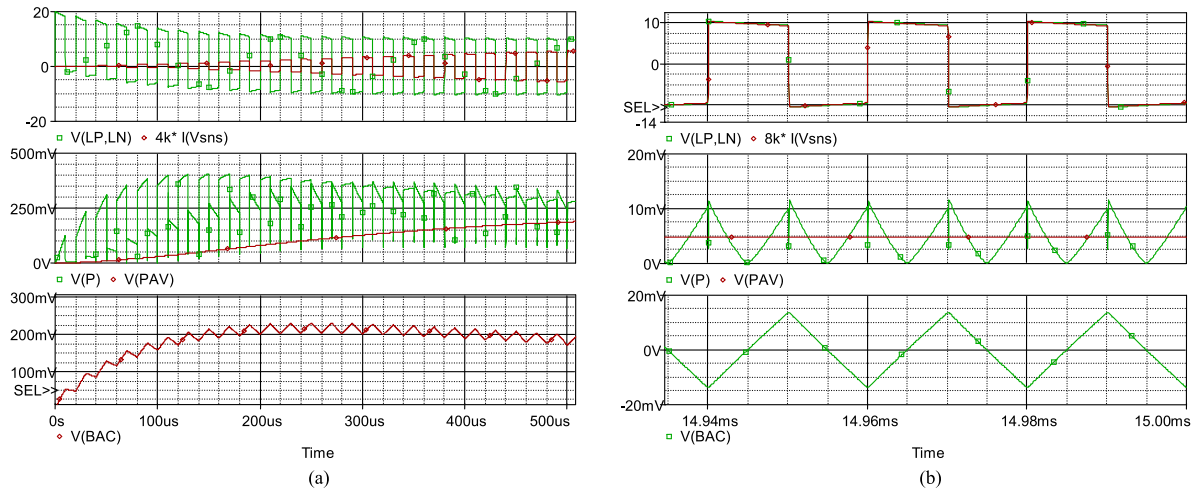

Fig. 5. (a) Typical simulation waveforms of RGSE power loss estimator under unipolar rectangular excitation: start-up transient; (b) steady-state. Upper screen– the inductor's voltage, *V*(*LP*,*LN*), and the scaled PCR current, 4*k***I*(*V*sns); middle screen- the instantaneous core power loss, *V*(*P*), and the average core power loss, V(PAV); bottom screen- the ac flux density, *V*(BAC).

screen shows the instantaneous core loss as predicted by RGSE, *V*(*P*), and the average core loss, V(PAV). The bottom screen shows the ac core flux density coded in voltage, *V*(BAC).

During the second series of software experiments RGSE-based algorithm was used to estimate the core losses under sinusoidal excitation and compare with a calculated replica of the SE core loss chart similar to the provided by ferrite cores manufacturers. The source voltage and frequency (20, 50, and 100 kHz) were adjusted, so as to generate the desired peak flux density (0.02, 0.05, and 0.08 T) in the CUT. The SE prediction was calculated based on (1), whereas the simulation results were obtained by SPICE applying the RGSE method described above. Comparison of the calculated losses versus SPICE simulated results are presented in Fig. 4(a). Absolute agreement of the results was found in all cases. This confirmed proper function of the RGSE power loss estimator.

During the third series of software experiments, the CUT was excited by a triangular flux density generated by a rectangular pulsed voltage with variable duty cycle. For any given duty cycle, the pulse amplitude was adjusted so to keep the peak flux density at 220 mT and with no dc offset. Hardware experiment on same core material and size was described in [10]. This allows us a comparison of the experimental results published earlier with present simulation results. Comparison of the measured core losses, reported by Reinert *et al.* [10], versus present SPICE simulated results is given in Fig. 4(b). Excellent agreement of the simulated and experimental results can be observed in the 0.5–0.9 duty cycle range, which, in fact, implies 0.1–0.9. The accuracy of RGSE prediction deteriorates at very high duty cycle ratio $D > 0.93$. Similar deterioration is expected for duty cycle lower than 0.7. However, since the extreme duty cycle regime is usually avoided in practice, the resulting error may not be of a great concern.

Comparison with the SE prediction can also be seen in Fig. 4(b). As can be observed, and presumably welcomed by practicing engineers, the simple SE provides acceptable estimation of core loss in a moderate duty cycle range.

During fourth software experiment the CUT was excited by unipolar rectangular voltage that resulted in triangular flux density with substantial dc offset similar to the situation in PWM converters. Simulated waveforms are shown in Fig. 5. Top screen portrays the inductor voltage, *V*(*Lp*,*Ln*), and the (magnified)

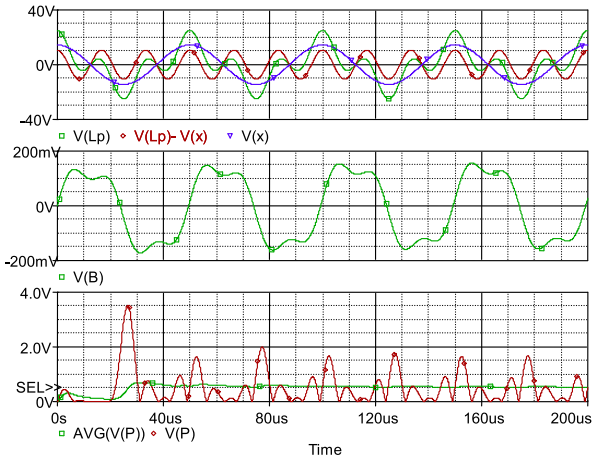

Fig. 6. Typical RGSE simulation waveforms under harmonically related sinusoidal excitation ($C = 0.2$). Upper screen – the low frequency source signal, $V(x)$, the triple harmonic source signal, $V(Lp)$–$V(x)$, and the resulting inductor's voltage, $V(Lp)$; middle screen- the core flux density, $V(B)$; bottom screen- the instantaneous core power loss, $V(P)$, and the average core power loss, AVG($V(P)$).

PCR current, $I(V\text{sns})$. Clearly, the PCR current reliably follows the waveform of the inductor's voltage, which implies correct emulation of resistive characteristic. The middle screen shows the instantaneous and the average core power loss predicted by RGSE. The bottom screen illustrates the ac flux density (coded in voltage), V(BAC).

The fifth series of software experiments was aimed to test how RGSE deals with flux density waveform that induces both major and minor loops. In order to do so, the CUT was excited by two harmonically related, in phase, sources so as to generate the flux density within the core according to

$$B\ (t)\ =\ 0.2\cdot\left((1-C)\sin\left(2\pi\cdot 20\cdot 10^3\cdot t\right)\right.$$
$$\left.+C\sin\left(2\pi\cdot 60\cdot 10^3\cdot t\right)\right). \qquad (14)$$

According to (13), the flux density amplitude of both sources can be varied by stepping the modulation parameter C in 0 to 1 range so that the peak flux density generated by the low frequency source reaches its maximum of 200 mT at $C = 0$, whereas the peak flux density generated by the high frequency source rises towards 200 mT at $C = 1$.

Same hardware experiment on same core material and size was described in [11]. Here the CUT was of the same material (3C85; $k = 12$, $k_1 = 4.523$, $a = 1.33$, $b = 2.55$), but had different geometry ($A_e = 117.4$ mm^2; $V_e = 10090$ mm^3) and different number of turns ($N = 6$).

Typical simulation waveforms for $C = 0.2$ are shown in Fig. 6. In the top screen, the excitation voltages are shown; the middle screen the resulting flux density, $V(B)$, is plotted; in the bottom screen the instantaneous, $V(P)$, and the average, AVG($V(P)$), RGSE power loss predictions can be seen.

Fig. 7 shows the comparison of the experimental results reported by Abdallah and Sullivan [11] versus the simulated results generated by RGSE-based SPICE program. The RGSE somewhat overestimates the loss in the $0.3< C <0.6$ range; however, on the whole, a good agreement of the results is observed. Excellent agreement is found at both high and low C range, where the flux density is dominated either by the higher frequency source, or by the low frequency source. Perfect match between the simulated and the experimental results is observed

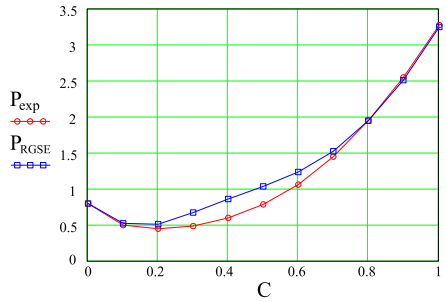

Fig. 7. Comparison of the simulated (P_{RGSE}) power loss prediction versus experimental results (P_{exp}) [11] under harmonically related (in phase) sinusoidal flux density components.

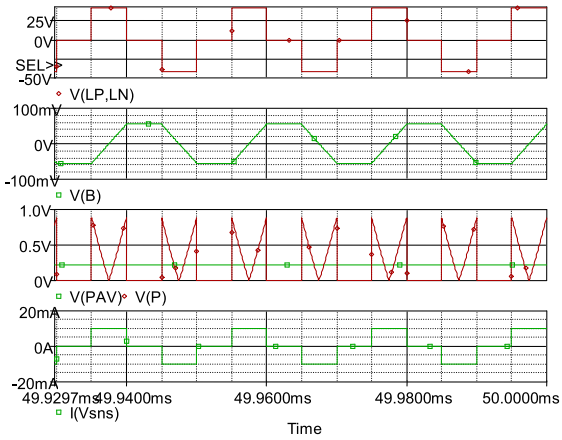

Fig. 8. Typical RGSE simulation waveforms of a DAB. Upper screen - inductor's voltage, $V(LP,LN)$; middle screen- core flux density, $V(B)$; bottom screen- the instantaneous core power loss, $V(P)$, and the average core power loss, V(PAV).

at the far edges of the plot where the flux density converges to a pure sinusoidal waveform (i.e., simple SE cases).

The last series of software experiments was aimed to test how RGSE estimates the losses in the transformer core of a typical double active bridge (DAB) converter. In DAB applications, the core might be subjected to rather long zero voltage excitation intervals, during which the relaxation effect takes place [14]. The software experiments reconstructed the hardware experiments of [14] as close as possible. The CUT winding was excited by a differential voltage between two phase shifted rectangular voltage sources each with amplitude of 42 V, and 50% duty cycle, running at 50 kHz. The phase shift was achieved by varying the time delay, t_d, between the pulses. The CUT parameters were EPCOS N87 R42, $k = 81.15$, $k_1 = 37.215$, $\alpha = 1.09$, $\beta = 2.16$, $l_e = 103$ mm, $A_e = 95.75$ mm^2, $V_e = 9862$ mm^3, and $N = 20$ turns.

Typical simulation waveforms of the CUT in the simulated DAB are shown in Fig. 8. Zero voltage intervals across the inductor winding and the typical trapezoidal flux density are clearly visible in the top and second screens. The third screen shows the instantaneous and time average power loss, whereas the bottom screen depicts the loss current component drown by the equivalent parallel resistance.

Fig. 9 shows a comparison between the experimental results reported by Muhlethaler *et al.* [14], and the simulated results generated by the RGSE-based SPICE program. Since the relaxation effect model is not incorporated into RGSE, RGSE

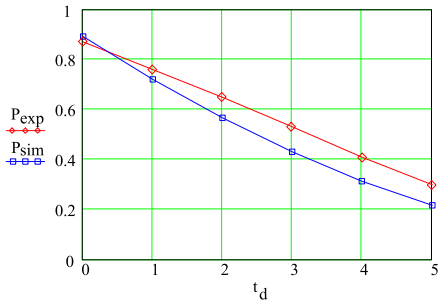

Fig. 9. Comparison of the simulated power loss ($P_{\rm sim}$) versus experimentally measured loss ($P_{\rm exp}$) [14] in the transformer core in a DAB as function of the zero voltage interval (time delay) t_d.

underestimates the core loss. Referred to the maximal power loss, the error is about 10%.

VI. Conclusion

This letter presented a SPICE methodology to estimate and simulate core power loss by the proposed RGSE model. The RGSE is a revision of the previously published GSE [11] loss model, which was shown to be a better fit to ferrite core losses than the original SE model. The improvement of the GSE over the SE is in the ability of the former to better handle nonsinusoidal magnetic flux excitation, and the fact that it does not require knowledge about the frequency of excitation. However, the earlier GSE model produced significant errors if the total magnetic flux excitation (ac plus dc) was used in calculations. The proposed RGSE overcomes the dc sensitivity by considering only the ac magnetic flux density, by subtracting the dc component beforehand. Thus, making the RGSE model insensitive to dc bias, this is an improvement over the earlier GSE model. However, for same reason, the RGSE model cannot account for dc bias inflicted loss. Except for the improvement of dc sensitivity, the RGSE is identical to the GSE and as such has inherited some other limitations of the latter and cannot properly account for neither the relaxation induced losses nor the temperature effects. Even so, the important advantage of RGSE model is that it can be used for calculating core power losses under arbitrary flux density waveform by just using the SPs and core geometry data. Another merit of the RGSE model is that it is SPICE friendly and can be easily adopted for simulation. The presented RGSE-based SPICE simulation approach can provide a reliable estimation of the core loss by analyzing the simulation data.

Comparison of the calculated and previously published results with the RGSE simulation results reveals excellent agreement in the sinusoidal case and good agreement in other cases. The simulation experiments of this study show that, barring extreme operating conditions (e.g., very short or very long duty cycles, or long relaxation times), the proposed RGSE simulation model was capable of making a quite accurate prediction of the experimental results.

It can, thus, be concluded that the proposed RGSE is a better model than the original SE and GSE models. Furthermore, the generic nature of the simulation model and the availability of the SPs, for just about any commercial core, make the proposed RGSE-based SPICE simulation approach an easy to use design tool.

References

[1] G. Bertotti, *Hysteresis in Magnetism: For Physicists, Materials Scientists, and Engineers*. San Francisco, CA, USA: Academic, 1998.

[2] H. N. Ji, Z. W. Lan, Z. Y. Xu, H. W. Zhang, J. X. Yu, and M. Q. Li, "Effects of second milling time on temperature dependence and improved Steinmetz parameters of low loss MnZn power ferrites," *IEEE Trans. Appl. Supercond.*, vol. 24, no. 5, Oct. 2014, Art. no. 7000104.

[3] W. A. Roshen, "A practical, accurate and very general core loss model for nonsinusoidal waveforms," *IEEE Trans. Power Electron.*, vol. 22, no. 1, pp. 30–40, Jan. 2007.

[4] Magnetics, "Magnetics Ferrites," 2017. [Online]. Available: https://issuu.com/magnetics/docs/magnetics_ferrite_catalog_2017

[5] TDK, "Ferrites and accessories," 2017. [Online]. Available: https://product.tdk.com/info/en/products/ferrite/index.html

[6] D. Y. Chen, "Comparison of the high frequency magnetic core losses under two different driving conditions: a sinusoidal voltage and a square-wave voltage," in *Proc. Int. Conf. IEEE Power Electron. Spec.*, New York, NY, USA, Jun. 1978, pp. 237–241.

[7] A. Van den Bossche, V. C. Valchev, and G. B. Georgiev, "Measurement and loss model of ferrites with non-sinusoidal waveforms," in *Proc. 2004 35th Annu. Conf. IEEE Power Electron. Spec.*, 2004, vol. 6, pp. 4814–4818.

[8] R. Garcia, A. Escobar-Mejía, K. George, and J. C. Balda, "Loss comparison of selected core magnetic materials operating at medium and high frequencies and different excitation voltages," in *Proc. 5th Int. Symp. IEEE Power Electron. Distrib. Gener. Syst.*, Jun. 2014, pp. 1–6.

[9] M. Albach, T. Durbaum, and A. Brockmeyer, "Calculating core losses in transformers for arbitrary magnetizing currents a comparison of different approaches," in *Proc. 27th Annu. Conf. IEEE Power Electron. Spec.*, Baveno, Italy, 1996, vol. 2, pp. 1463–1468.

[10] J. Reinert, A. Brockmeyer, and R. De Doncker, "Calculation of losses in ferro- and ferrimagnetic materials based on the modified Steinmetz equation," *IEEE Trans. Ind. Appl.*, vol. 37, no. 4, pp. 1055–1061, Jul./Aug. 2001.

[11] J. Li, T. Abdallah, and C. R. Sullivan, "Improved calculation of core loss with non-sinusoidal waveforms," in *Proc. 36th Int. Conf. IEEE IAS Ind. Appl.*, 2001, vol. 4, pp. 2203–2210.

[12] K. Venkatachalam, C. R. Sullivan, T. Abdallah, and H. Tacca, "Accurate prediction of ferrite core loss with non-sinusoidal waveforms using only Steinmetz parameters," in *Proc. Int. Conf. IEEE Comput. Power Electron.*, 2002, pp. 36–41.

[13] H. E. Tacca and C. R. Sullivan, "Extended Steinmetz equation (ESE)," 2002. [Online]. Available: https://www.aacademica.org/hernan.emilio.tacca/2.pdf.

[14] J. Muhlethaler, J. Biela, J. W. Kolar, and A. Ecklebe, "Improved core-loss calculation for magnetic components employed in power electronic systems," *IEEE Trans. Power Electron.*, vol. 27, no. 2, pp. 964–973, Feb. 2012.

[15] J. Muhlethaler, J. Biela, J. W. Kolar, and A. Ecklebe, "Core losses under the DC bias condition based on Steinmetz parameters," *IEEE Trans. Power Electron.*, vol. 27, no. 2, pp. 953–963, Feb. 2012.

[16] C. R. Sullivan, J. H. Harris, and E. Herbert, "Core loss predictions for general PWM waveforms from a simplified set of measured data," in *Proc. 2010 25th Annu. Conf. IEEE Appl. Power Electron.*, Palm Springs, CA, USA, 2010, pp. 1048–1055.

[17] M. Mu and F. C. Lee, "A new core loss model for rectangular AC voltages," in *Proc. 2014 Int. Conf. IEEE Energy Convers. Congr.*, Pittsburgh, PA, USA, 2014, pp. 5214–5220.

[18] R. Ridley and A. Nace, "Modeling Ferrite core losses," Switching Power Magazine, 2006. [Online]. Available: https://www.academia.edu/25540300/Modeling_Ferrite_Core_Losses

[19] M. H. F. Lim and J. D. van Wyk, "Applying the steinmetz model to small cores in LTCC ferrite for integration applications," in *Proc. 2009 24th Annu. Conf. IEEE Appl. Power Electron.*, Washington, DC, USA, 2009, pp. 1027–1033.

[20] S. Barg, K. Ammous, H. Mejbri, and A. Ammous, "An improved empirical formulation for magnetic core losses estimation under nonsinusoidal induction," *IEEE Trans. Power Electron.*, vol. 32, no. 3, pp. 2146–2154, Mar. 2017.

[21] A. J. Marin-Hurtado, S. Rave-Restrepo, and A. Escobar-Mejía, "Calculation of core losses in magnetic materials under nonsinusoidal excitation," in *Proc. 2016 13th Int. Conf. Power Electron.*, Guanajuato, Mexico, 2016, pp. 87–91.

[22] PSPICE User's Guide, Version 4.00, MicroSim Corp., Jan. 1989.

[23] C. E. Hymowitz, "Power Specialist's App Note Book," Intusoft Corp., 1998. [Online]. Available: http://www.i-vis.co.jp/pdf/intusoft/app/psbook.pdf